1-2014

High Resolution Time-of-Flight Mass Spectrometry Fingerprinting of Metabolites from Cecum and Distal Colon Contents of Rats Fed Resistant Starch

Timothy James Anderson
Iowa State University, timma@iastate.edu

Roger W. Jones
Iowa State University, jonesrw@ameslab.gov

Yongfeng Ai
Iowa State University

Robert S. Houk
Iowa State University, rshouk@iastate.edu

Jin Jane
Iowa State University, jjane@iastate.edu

See next page for additional authors

High Resolution Time-of-Flight Mass Spectrometry Fingerprinting of Metabolites from Cecum and Distal Colon Contents of Rats Fed Resistant Starch

Abstract
Time-of-flight mass spectrometry along with statistical analysis was utilized to study metabolic profiles among rats fed resistant starch (RS) diets. Fischer 344 rats were fed four starch diets consisting of 55 % (w/w, dbs) starch. A control starch diet consisting of corn starch was compared against three RS diets. The RS diets were high-amylose corn starch (HA7), HA7 chemically modified with octenyl succinic anhydride, and stearic-acid-complexed HA7 starch. A subgroup received antibiotic treatment to determine if perturbations in the gut microbiome were long lasting. A second subgroup was treated with azoxymethane (AOM), a carcinogen. At the end of the 8-week study, cecal and distal colon content samples were collected from the sacrificed rats. Metabolites were extracted from cecal and distal colon samples into acetonitrile. The extracts were then analyzed on an accurate-mass time-of-flight mass spectrometer to obtain their metabolic profile. The data were analyzed using partial least-squares discriminant analysis (PLS-DA). The PLS-DA analysis utilized a training set and verification set to classify samples within diet and treatment groups. PLS-DA could reliably differentiate the diet treatments for both cecal and distal colon samples. The PLS-DA analyses of the antibiotic and no antibiotic-treated subgroups were well classified for cecal samples and modestly separated for distal colon samples. PLS-DA analysis had limited success separating distal colon samples for rats given AOM from those not treated; the cecal samples from AOM had very poor classification. Mass spectrometry profiling coupled with PLS-DA can readily classify metabolite differences among rats given RS diets.

Keywords
resistant starch, mass spectrometry, metabolites, PLS-DA

Comments
This is a manuscript of an article in *Analytical and Bioanalytical Chemistry* 406 (2014): 745. Posted with permission. The final publication is available at Springer via http://dx.doi.org/10.1007/s00216-013-7523-8.

Authors
Timothy James Anderson, Roger W. Jones, Yongfeng Ai, Robert S. Houk, Jay-lin Jane, Yinsheng Zhao, Diane F. Birt, and John Frederick McClelland

The article is from *Analytical and Bioanalytical Chemistry* 406 (2014): 745. Posted with permission. The final publication is available at Springer via http://dx.doi.org/10.1007/s00216-013-7523-8.

High Resolution Time-of-Flight Mass Spectrometry Fingerprinting of Metabolites from Cecum and Distal Colon Contents of Rats Fed Resistant Starch

Timothy J. Anderson,[1,2] Roger W. Jones,[1] Yongfeng Ai,[3] Robert S. Houk,[1,2] Jay-lin Jane,[3] Yinsheng Zhao,[3] Diane F. Birt,[3] John F. McClelland[1,4]

[1]Ames Laboratory-USDOE, Iowa State University, Ames, IA 50011, USA
[2]Department of Chemistry, Iowa State University, Ames, IA 50011, USA
[3]Department of Food Science and Human Nutrition, Iowa State University, Ames, IA 50011, USA
[4]Department of Mechanical Engineering, Iowa State University, Ames, IA 50011, USA

Abstract: Time-of-flight mass spectrometry along with statistical analysis was utilized to study metabolic profiles among rats fed resistant starch (RS) diets. Fischer 344 rats were fed four starch diets consisting of 55% (*w*/*w*, dsb) starch. A control starch diet consisting of corn starch was compared against three RS diets. The RS diets were high-amylose corn starch (HA7), HA7 chemically modified with octenyl succinic anhydride, and stearic-acid-complexed HA7 starch. A subgroup received antibiotic treatment to determine if perturbations in the gut microbiome were long lasting. A second subgroup was treated with azoxymethane (AOM), a carcinogen. At the end of the 8-week study, cecal and distal colon contents samples were collected from the sacrificed rats. Metabolites were extracted from cecal and distal colon samples into acetonitrile. The extracts were then analyzed on an accurate-mass time-of-flight mass spectrometer to obtain their metabolic profile. The data were analyzed using partial least-squares discriminant analysis (PLS-DA). The PLS-DA analysis utilized a training set and verification set to classify samples within diet and treatment groups. PLS-DA could reliably differentiate the diet treatments for both cecal and distal colon samples. The PLS-DA analyses of the antibiotic and no antibiotic-treated subgroups were well classified for cecal samples and modestly separated for distal colon samples. PLS-DA analysis had limited success separating distal colon samples for rats given AOM from those not treated; the cecal samples from AOM had very poor classification. Mass spectrometry profiling coupled with PLS-DA can readily classify metabolite differences among rats given RS diets.

Keywords: Resistant Starch, Mass Spectrometry, Metabolites, PLS-DA

Introduction

Food is composed of three main components, which are protein, lipid and starch. Cereal grains are one of the world's most important food sources; of these, its most abundant component is typically starch. Amylopectin and amylose make up the bulk of starch granules; their relative concentration can vary depending on source material. Amylopectin comprises

typically about 70 % of the starch granule but can reach 100 % for waxy corn varieties. Amylose levels are typically about 15–30 % of the starch granule [1-3].

Both amylopectin and amylose are comprised of polymeric glucose. Recent studies have shown that amylose forms double helical structures, and the hydroxyl groups of the individual glucose units may be esterified with a variety of lipid-like compounds [3]. Amylose can also form single helical complexes with free fatty acids and iodine. These modified amylose structures along with food materials that contain up to 85 % amylose are examples of resistant starch (RS) [3], which effectively resist digestion in the stomach and small intestine, and thus are processed farther along the gut [4].

RS has been studied for a variety of health benefits. RS may aid diabetics, decrease energy density, and also act as a prebiotic [5-10]. Prebiotics are materials which resist digestion by the host and are metabolized in the gut by microorganisms [10]. The microorganisms release compounds, such as short-chain fatty acids, which are believed to be beneficial to the host organism [11, 12]. The interplay between microorganisms and host is complex; the microorganisms may even interact with host diet to increase deleterious conditions such as intestinal inflammation [13]. Some materials, such as oligofructose, lactulose, and transgalacto-oligosaccharides are well characterized and known to be prebiotics, but only recently has RS been classified as a prebiotic [14-20].

The catabolism of prebiotics by microorganisms produces a vast array of chemical components, which are classified as metabolites [21]. Metabolites from gut microorganisms can be obtained from blood, urine, or feces [22-24]. Blood and urine reflect metabolic changes that occur in the gut from direct absorption through the intestinal lining [25, 26]. Feces are complex media from which a direct interplay between microorganism and host can be observed [27].

There are five RS categories. Whole grains and ground legumes contain type 1 RS. Type 1 RS is amylose protected by cell wall material and other plant materials that are difficult to digest. Type 2 RS retains a crystalline structure, which resists enzyme hydrolysis, and is found primarily in banana and potato starch. Type 3 RS is retrograded starch; this occurs when the starch granule has gelatinized and reformed a crystalline structure [28]. Type 4 RS is a chemically modified starch molecule. To produce the type 4 RS, a lipid compound such as octenyl succinic anhydride is generally bound to the various hydroxyl groups of glucose within the starch amylose molecule [14, 29]. Type 5 RS is formed from a physical interaction of debranched helical starch amylose and a long chain fatty acid, such as palmitic or stearic acid [30].

Mass spectrometry has emerged as one of the most important platforms for metabolite analysis due to improvements in ionization methodology and high-resolution instruments. A variety of metabolite separation methods can be coupled with mass spectrometers. The coupling allows comprehensive analysis through fingerprinting or profiling of metabolites [31, 32]. Gas chromatography-mass spectrometry (GC-MS) is useful for the analysis of thermally stable volatile compounds. GC-MS often utilizes electron impact (EI) ionization. The GC separation and subsequent EI fragmentation often allow metabolite identification through database searching [27, 33-35]. Liquid chromatography-mass spectrometry (LC-MS) is very useful for metabolite analysis because specialized columns can be used to separate either polar or non-polar compounds [25, 26, 36]. LC-MS can also be coupled with collision induced dissociation that provides fragment ions for potential metabolite identification [28, 37]. Capillary electrophoresis (CE) is another separation technique that can be used prior to mass spectrometry analysis [38, 39]. Work performed with CE and LC-MS has attempted to identify metabolites using standard

retention time libraries and elemental formulas from accurate mass measurements [40]. Ultra-high resolution mass spectrometry using Fourier transform ion cyclotron resonance instruments has been used for metabolite analysis [41, 42]. Even matrix-assisted laser desorption ionization imaging has recently been coupled with mass spectrometry to obtain metabolite insight [43].

Statistical tools have become important in the postexamination of metabolites analyzed using mass spectrometry. Tools such as principal component analysis, soft independent modeling of class analogy, partial least-squares discriminant analysis (PLS-DA), linear discriminant analysis, and artificial neural networks all allow differentiation and group prediction [26, 27, 34, 35, 39, 44-46]. Using these tools, difficult and complex analyses of large amounts of data can be more easily graphed and visualized.

The current study describes such methods for profiling the metabolites from rat cecal and distal colon contents to deduce differences among RS diets. Three different RS and a control corn starch were fed to rats. The first RS was a type 2 RS that consisted of high amylose corn starch (HA7). The second RS was a type 4 RS that was HA7 corn starch modified with octenyl succinic anhydride (OS-HA7). The last RS was a type 5 RS that was produced by complexing HA7 with stearic acid (StA-HA7). The main goal of this study was to determine whether statistical tools, such as PLS-DA, could observe differences among RS starch diets from rat cecal and distal colon contents using mass spectrometry. Another goal was to understand whether statistical tools could accurately group diets and target their individual biomarkers that vary the most among the diets.

Materials and methods

Animal study

Male Fischer 344 rats were housed and fed according to the procedure of Zhao et al. [47]. The study initially used 90 rats (two died before sacrifice) that were obtained at 5 weeks old and were placed on specific feeding regimens for 8 weeks, as shown in the flow diagram in Fig. 1. The animals were randomly separated into four starch diet groups: Control, HA7, OS-HA7, and StA-HA7. The control and StA-HA7 starch diet groups each had 29 rats, and both diets contained four further subgroup treatments. Rats fed HA7 and OS-HA7 starch diets had 15 rats each, and both diets contained only two further subgroup treatments. All four starch diet groups were divided into two treatment subgroups, which consisted of 9–10 rats given either two injections of the carcinogen azoxymethane (AOM, Midwest Research Institute, Kansas City, MO, USA) at a dose of 20 mg AOM/kg rat body weight and 4–5 rats given two injections of saline administered 8 weeks prior to sample collection, following the method of Zhao et al. [47]. In the control and StA-HA7 diet groups, both of the injection subgroups were further split into two more subgroups consisting of rats either administered an antibiotic consisting of a combination of imipenem and vancomycin at a dose of 50 μg/mL each in the drinking water in week 2 (Fig. 1) or not administered any antibiotic.

Starch diet materials

Normal corn starch (NCS, Cargill Gel™) and HA7 (AmyloGel™) were purchased from Cargill Inc. (Minneapolis, MN, USA), 2-octen-1-ylsuccinic anhydride (OSA), pullulanase

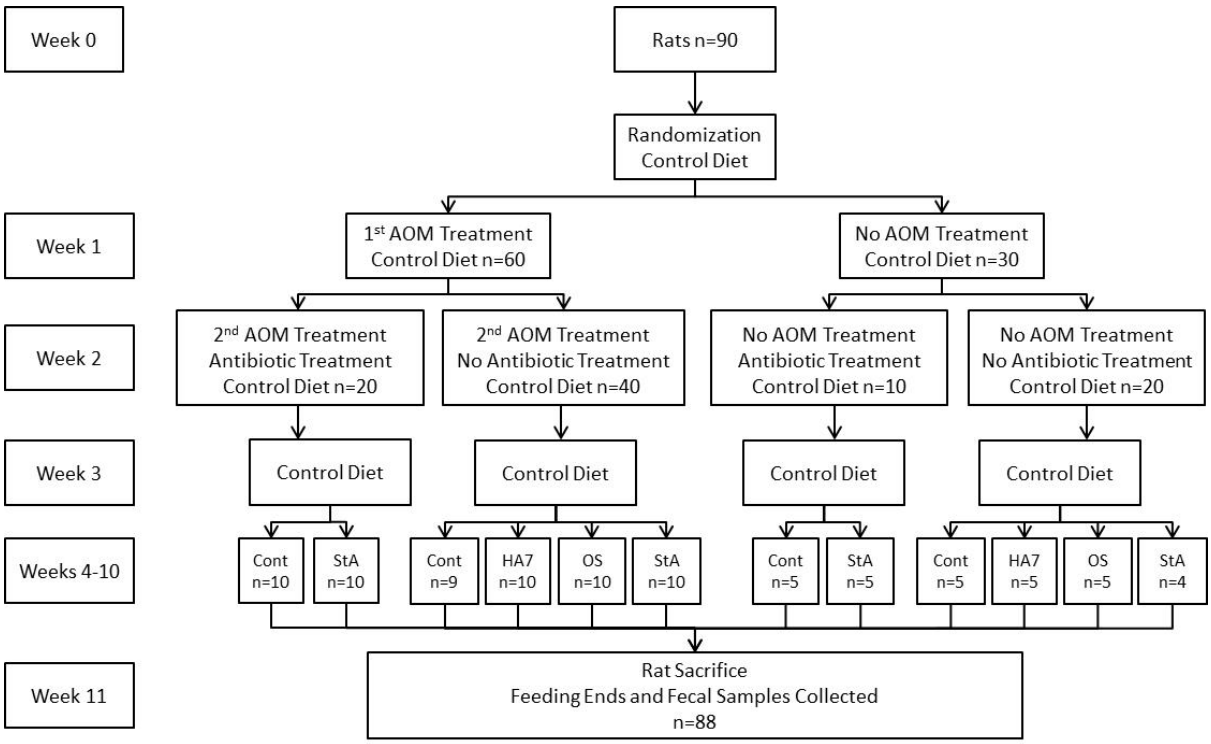

Fig. 1 Flow diagram of the animal study detailing the treatment schedule for AOM, antibiotic, and diet up until sacrifice. The diets that were given for weeks 4-10 are represented as the abbreviations *cont* (Control), *HA7* (HA7), *OS* (OS-HA7), and *StA* (StA-HA7). The amount of rats in each group of the flow chart are represented by the letter "*n*"

from *Bacillus acidopullulyticus* and stearic acid (SA) were purchased from Sigma-Aldrich Co. (St. Louis, MO, USA). All starch was cooked prior to addition to the rat diets, in accordance with the procedure of Zhao et al. [47]. The nonstarch component of the rat diet was prepared in compliance with the standards of the American Society for Nutritional Sciences for mature rats (AIN-93M) [48]. The diets were prepared every other day and served fresh to the rats.

Preparation of OS-HA7 starch diet

OS-HA7 was produced from the HA7 through modification with OSA [49]. The HA7 was suspended in water at a concentration of 35 % (*w*/*w*, dsb). The pH of the starch slurry was adjusted to 8.0 by adding a sodium hydroxide aqueous solution (3 %, *w*/*w*), and the temperature was maintained at 35 °C. OSA (10 %, *w*/*w*, dsb) was added to the slurry dropwise while maintaining the pH at 8.0 and 35 °C. After the reaction was completed, the pH of the starch slurry became stable and was then adjusted to 6.5 by adding 1.0 M hydrochloric acid. The starch was recovered using filtration, washed with distilled water and 100 % ethanol, dried at 37 °C, and then ground to fine powder.

Preparation of StA-HA7 starch diet

StA-HA7 was prepared from the HA7 following the method of Hasjim et al. [30] with modifications. The HA7 was suspended in water at a concentration of 10 % (*w*/*w*, dsb). The

starch slurry was pre-heated to 80 °C, and the temperature maintained for 1 h with stirring. Pullulanase (5 U/g starch, dsb) was added to the slurry to hydrolyze α 1-6 branch linkages of the starch at 60 °C for 24 h. Stearic acid (SA, 10 %, *w*/*w*, dsb) was added, and the mixture was kept at 80 °C for 1 h with vigorous stirring for amylose-SA complex formation. After cooling to room temperature, the StA-HA7 was recovered using centrifugation, washed with 50 % (*v*/*v*) aqueous ethanol solution, dried at 37 °C, and then ground.

Rat cecal samples

The rat cecum was removed just after sacrifice. The cecum contents were placed in 15-mL centrifuge tubes (Corning, Tewksbury, MA, USA) and stored on dry ice until placed in long term storage at -80 °C. Of the 88 rats sampled, 81 cecal samples were analyzed. For control, HA7, OS-HA7, and StA-HA7 diets, 24, 15, 14, and 28 samples were analyzed, respectively. The lower number of samples analyzed for the control diet was due to reduced sample volume. All RS fed rats had ceca of substantial size; on average they were nearly four times the mass of the control.

Rat distal colon samples

After sacrifice, the rat colon was opened. Fecal pellets were collected from the large intestine starting from the anus to 5 cm up the colon and were placed in 15-mL centrifuge tubes containing phosphate buffer. The samples were placed on dry ice, and then stored long term at -80 °C. Seventy-two distal colon samples were analyzed from the original 88 rats. From control, HA7, OS-HA7, and StA-HA7 diets, 22, 13, 11, and 26 samples were analyzed, respectively. The drop in samples analyzed in respect to cecum samples was due to random amounts of fecal pellets in the colon. Some rats contained many pellets, while some had none at the time of sacrifice.

Metabolite extraction for cecal and distal colon samples

The metabolite extraction was an adaption of the method of Antunes et al. [42]. Frozen cecal and distal colon samples were thawed and approximately 150 mg of sample was placed in a 2.0-mL microcentrifuge tube (Eppendorf, Hamburg, Germany). The tube was then half-filled with 1 mm zirconia/silica beads (Biospec Products, Bartlesville, OK, USA) and 1 mL of HPLC grade acetonitrile (Fischer Scientific, Fair Lawn, NJ) was introduced. The microcentrifuge tubes were placed on a vortex apparatus (Fisherbrand, Bohemia, NY, USA) with an orbital bead homogenizing adaptor (Mo Bio Laboratories Inc., Carlsbad, CA, USA). The samples were vortexed until homogenized. The liquid portion of each sample was then pipetted into a clean microcentrifuge tube. The samples were placed in a centrifuge (Model 5415C, Eppendorf, Westbury, NY, USA) for 5 min at 12,000 rpm. From the centrifuge tube, 500 µL of supernatant was placed in a clean centrifuge tube, then vacuum centrifuged (Labconco Corporation, Kansas City, MO, USA) at 50 °C and depressurized with a dry vacuum pump (Welch Rietchle Thomas, Skokie, IL, USA). The dried metabolite extracts were stored at -20 °C.

The dried metabolite extracts were reconstituted for mass spectrometry analysis by adding 500 µL of a 60 % (*v*/*v*) aqueous acetonitrile solution. The extract was vigorously vortexed and then centrifuged for 2 min at 12,000 rpm. One hundred microliters of supernatant

was removed and placed in a clean microcentrifuge tube. An additional 500 µL of 60 % (*v*/*v*) aqueous acetonitrile was added to dilute the sample. Formic acid was added to produce a 0.2 % formic acid sample solution to aid in positive ion production by electrospray ionization (ESI). Lastly, the solution was vortexed and transferred into 12- × 35-mm clear glass vials to be placed in an LC autosampler.

Mass Spectrometry

From the reconstituted cecal and distal colon metabolite extracts, 20 µL of sample was injected into an Agilent 1260 Infinity LC system (Agilent Technologies, Inc., Santa Clara, CA, USA), which was used as an autosampler. The samples were direct-infused from the LC and ionized using ESI in positive mode on an Agilent 6224 time-of-flight mass spectrometer operated at an acquisition rate of 4 GHz. A sample run lasted 5 min with a mobile phase of 60 % (*v*/*v*) aqueous acetonitrile. A second mobile phase of 60 % (*v*/*v*) aqueous acetonitrile with 20 ppm of a 50:50 mixture of polyethylene glycol (PEG) 200 and 600 standards (Hampton Research, Aliso Viejo, CA, USA) was used for calibration. At 48 s into a sample run, the PEG-containing mobile phase was used for 12 s. At 1 min, the primary mobile phase was switched inline and flushed the PEG calibrant from the system prior to the next sample.

The software used was Agilent MassHunter Qualitative Analysis. Each spectrum was background subtracted, and the *m*/*z* scale was recalibrated using 17 ammoniated PEG-adduct peaks ranging from *m*/*z* 168.1236 to 872.5430. The calibrated spectra were centroided and exported as text files. The text files for each diet and subgroup were averaged using custom software. The averaged text files were then uploaded to the MassTRIX website, and accurate mass data were compared to rat metabolites in the KEGG database [50].

Statistical analysis

Separate PLS-DA classification models were developed using commercial software (Pirouette Version 4.5; Infometrix, Inc.; Bothell, WA, USA) for diet, AOM treatment, and antibiotic treatment. The cecal and distal fecal datasets were modeled separately. The cecal and distal fecal datasets consisted of spectra from 81 and 72 rats, respectively. These sets included data from AOM-treated and antibiotic-treated rats, as well as untreated ones. The verification set consisted of 25 % of the total number of samples, and the remaining 75 % of samples were placed in the training set. The verification set was comprised of as close to one quarter of diet, AOM, and antibiotic treated samples as possible to ensure equal weighting during classification. The appropriate number of rats from each treatment was randomly selected for the verification set without previous knowledge of the spectral results. Each spectrum was normalized so that the base peak had an intensity of 100. Small peaks with intensities below one were then eliminated. The data were aligned using a mass tolerance of 0.005 *m*/*z* so that peaks in different spectra within a range of *m*/*z* ~ 0.010 were assigned the same (average) mass. In PLS-DA, each training-set spectrum is assigned a class-fit value of one for any class to which its sample belongs and a class-fit value of zero for classes to which its sample does not belong. When the verification set is analyzed, the resulting model determines the class-fit values of each spectrum for every class. Each verification-set spectrum is then assigned to the class for which its class-fit

value is closest to one, which usually means the one class for which its class-fit value is above 0.5.

Prior to modeling, the spectra were always mean-centered and for some models one-component orthogonal signal correction was used [51]. The resulting regression vectors for the classes (e.g., diets) were used to identify those peaks that most strongly differentiate the classes, and the corresponding species were examined as possible biomarkers.

Results and discussion

Mass spectrometry

Even without the mass spectrometry analysis, there were obvious differences in the digestive-tract contents of rats fed different diets. As described previously, the RS fed rats had ceca, which were as much as four times greater in mass than the rats on the control diet. The increased mass may have been due to increased fermentation time in the cecum to obtain nutrients from resilient RS components. The color, consistency, and aroma of the cecal contents were much different for the control compared to the RS diets. These differences may be linked to the amount of the starch fermented and thus tied to the gut microorganisms and metabolites. The primary difference among distal colon contents was that the various diets had distinct colors.

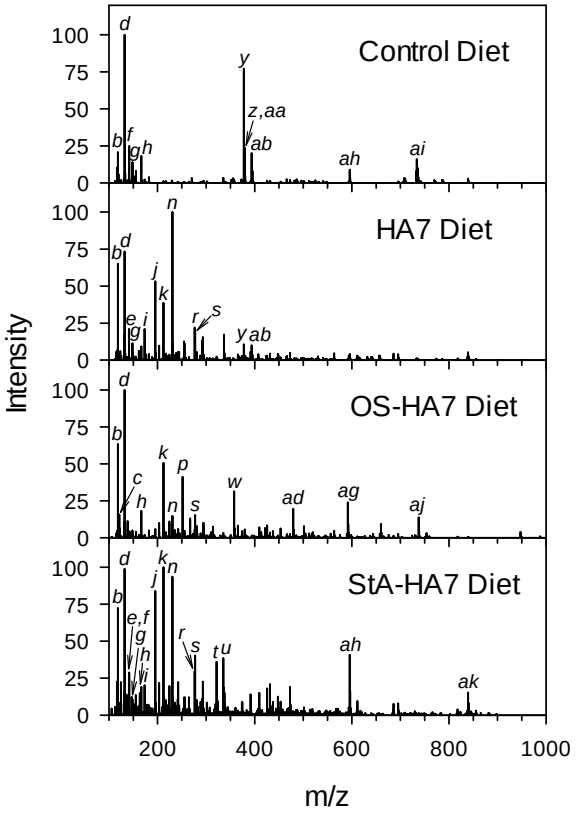

Fig. 2 Averaged mass spectra of cecal content samples from each diet group with no AOM or antibiotic treatments. The peak intensities have been normalized against the strongest peak in the spectrum for each diet. The most prominent metabolite peaks in each diet have been labeled and can be matched to their respective *m*/*z* in Table 1

Mass spectra of metabolites from the cecal contents of rats that were fed with different diets and received no AOM or antibiotic were averaged and are compared in Fig. 2. The main emphasis of the study was to determine differences among diets in respect to their metabolite profiles. A metabolite peak was considered specific to a diet group if the peak was approximately three times the intensity of the same peak in the other diets. The peaks are given letter labels in the figure, and Table 1 lists their *m*/*z* values and the diets in which they were found. First, the peaks that were specific to only one diet group were inspected. The control group had four specific peaks labeled *y*, *z*, *aa*, and *ai*. The HA7 group had no specific peaks. The OS-HA7 group contained six specific peaks marked *c*, *p*, *w*, *ad*, *ag*, and *aj*. The last group, StA-HA7, had four specific peaks labeled *t*, *u*, *ah*, and *ak*. Far fewer metabolite peaks were shared between any two of the groups. The *ab* peak was shared by the control and HA7 groups. Another peak, labeled *f*, was in both the control and StA-HA7 groups. The HA7 and StA-HA7 groups had five mutual peaks marked *e*, *i*, *j*, *n* and *r*. Fewer peaks were observed among three common groups. The control, HA7, and StA-HA7 diets shared the *g* peak. The control, OS-

HA7, and StA-HA7 diets contained a single peak in common, labeled *h*. The HA7, OS-HA7 and StA-HA7 diet groups shared the three peaks *b*, *k* and *s*. Only one prominent metabolite was observed in all groups; it was the *d* peak.

Mass spectra of the diet treatment metabolites in the distal colon contents are compared in Fig. 3. Similarly to the cecal contents, the mass spectra for the distal colon contents were averaged from rats that received no AOM or antibiotic. The peaks were also classified as specific to diet groups if they were approximately three times the intensity of the other diet groups. Like the labeled cecal-contents peaks in Fig. 2, further information about the lettered peaks in Fig. 3 can be found in Table 1. No peaks were observed to be specific to the control group. The HA7 group had only one exclusive peak, labeled *af*. The OS-HA7 group had seven peaks—*m*, *p*, *q*, *w*, *ad*, *ae*, and *aj*. Lastly, StA-HA7 had the six peaks *k*, *l*, *o*, *t*, *ac*, and *ak*. Fewer metabolite peaks were shared between any two groups than the peaks specific to a single group. The control and StA-HA7 diet groups shared the four peaks *a*, *g*, *x* and *ah*. The HA7 and StA-HA7 diets contained five common peaks—*j*, *n*, *r*, *s*, and *v*. Only the metabolite *h* was shared among the control, OS-HA7, and StA-HA7 diet groups. The two peaks *b* and *d* were shared among all four diet groups.

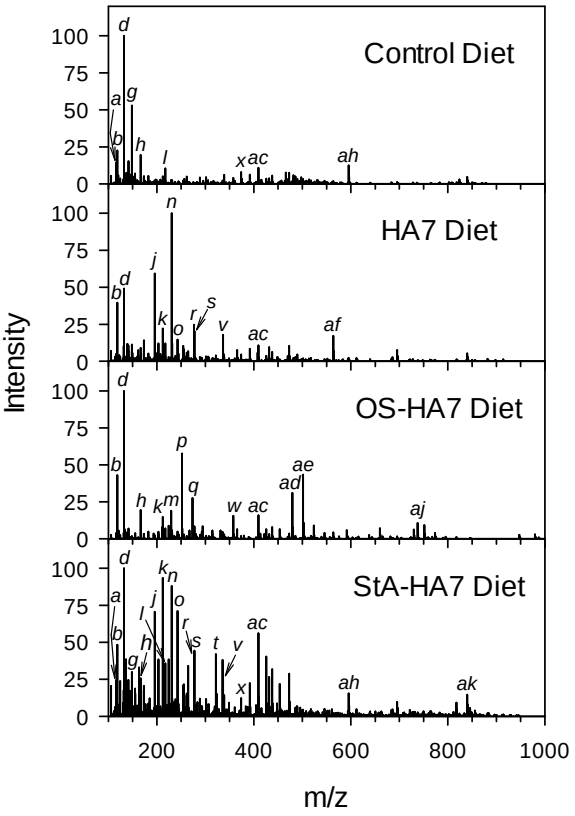

Fig. 3 Averaged mass spectra of distal colon content samples from each diet group with no AOM or antibiotic treatments. The peak intensities have been normalized against the strongest peak in the spectrum for each diet. The most prominent metabolite peaks in each diet have been labeled and can be matched to their respective *m*/*z* in Table 1

Analysis of the mass spectra in Figs. 1 and 2 highlighted modest differences between the cecal and distal colon contents. Spectra for the control and StA-HA7 diet group for both digestive locations have been placed in Fig. 4 for comparison. Specific peaks across digestive locations for a diet group were chosen with the same rule as described above for Figs. 2 and 3, and the peaks are again identified in Table 1. The control group for the cecal contents contained peaks labeled *y*, *z*, *aa*, *ab*, and *ai*, which were more intense than the same peaks in the distal colon contents. The distal colon contents contained the four peaks labeled *g*, *l*, *x*, and *ac*, which were more intense than those same peaks observed in the cecal contents. Both digestive locations shared the peaks *a*, *b*, *d*, *f*, *h*, and *ah* with similar intensities. The StA-HA7 group for both cecal and distal colon digestive locations was more complex than the control group. The cecal contents contained only one peak, labeled *ah*, that was more intense than in the distal colon contents. Peaks *g*, *l*, *o*, and *ac* had higher intensities in the distal colon contents than in the cecal contents. Peaks labeled *a*, *b*, *d*, *f*, *h*, *j*, *k*, *n*, *r*, *s*, *t*, *u* and *ak* were at similar intensities in the cecal and distal colon contents.

From this scrutiny of the mass spectra of the cecal contents and distal colon contents for the diets, it is apparent that RS diets altered the metabolism of the rats. In Table 1 the cecal contents from each diet had a distinct metabolite profile. Of the 27 labeled metabolites, 52 % were specific to only one diet group. These differences among diets persisted into the distal colon contents, for which 54 % of the 26 labeled metabolites in Table 1 were exclusive to individual diet groups. Figure 4 compared the cecal and the distal colon contents of the control diet, Table 1 described that 77 % of the 13 labeled metabolites are specific to one or the other digestive location. Figure 4 also compared spectra of cecal and distal colon contents of the StA-HA7 diet, and 22 metabolites from Table 1 were specific to only 45 % of either digestive location. For the control, there appears to be substantial change to the metabolite profile. However, for RS, such as StA-HA7, there was less variability in the metabolite profile from cecum to distal colon.

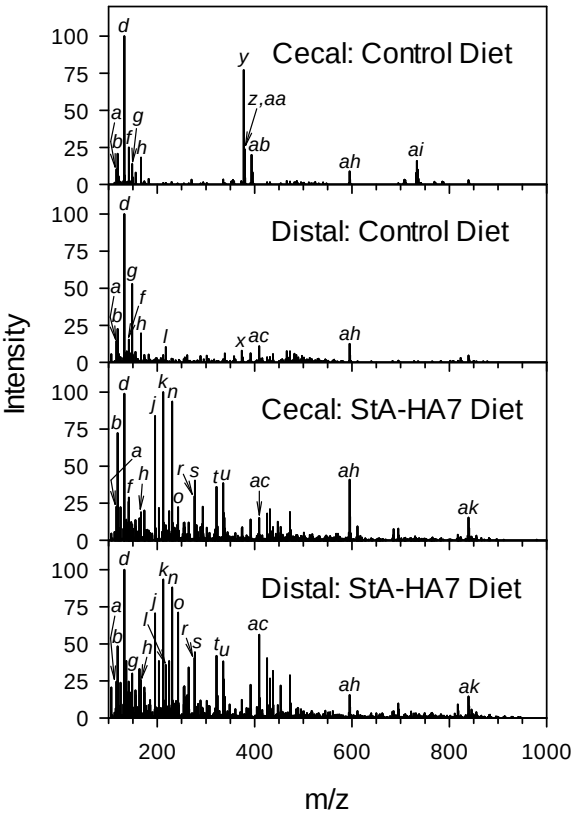

Fig. 4 Averaged mass spectra comparison of cecal and distal colon content samples from two example diets with no AOM or antibiotic treatments. The peak intensities have been normalized against the strongest peak in the spectrum for each diet. The most prominent metabolite peaks in the spectra have been labeled and can be matched to their respective *m*/*z* in Table 1

In a companion study to this one that used the same samples, Anderson et al. [52] determined through enzymatic assay that the average cecal starch content (dsb) for the control, HA7, OS-HA7, and StA-HA7 diets were 0.7, 18.3, 48.8, and 21.9 %, respectively. The residual starch differences are most likely attributed to the ability of each starch to be fermented in the cecum. The control and OS-HA7, which were the most and least fermented diets, respectively, had more diet-specific metabolites for both cecal and distal contents. The HA7 and StA-HA7 RS diets had nearly the same degree of fermentation and also shared many metabolites in the cecal and distal colon contents. The HA7 and StA-HA7 similarities also could be due to the relationship between the diets; StA-HA7 was produced from a complex of HA7 and stearic acid, and StA-HA7 may share some of the fermentation products of its parent RS. Regardless, the degree of fermentation and the nature of the starch source are probably the largest factors regarding the divergence of the metabolite profiles.

Statistical analysis of cecal contents

Classification analysis of the mass spectra for the RS diet groups was performed with PLS-DA for the cecal extracts. PLS-DA modeling was done for the cecal contents with a 61 sample training set, and a 20 sample verification set. The verification set contained six, four,

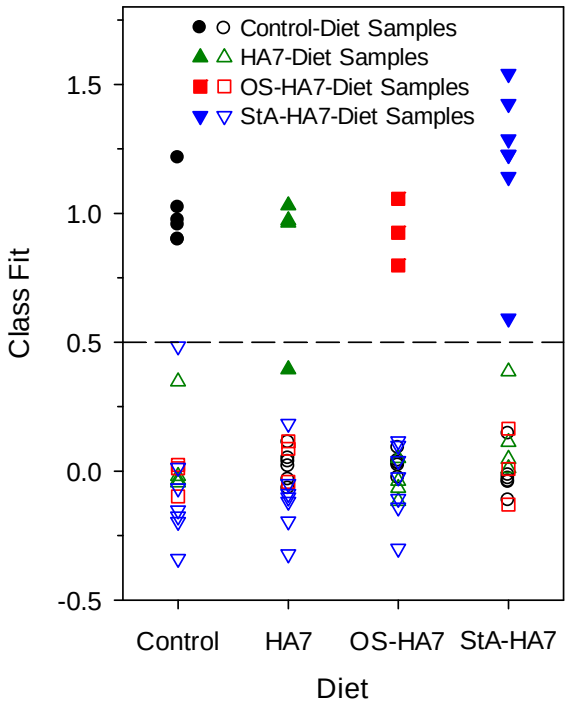

Fig. 5 PLS-DA analysis of cecal-content verification-set samples for diet treatments, including AOM- and antibiotic-treated samples. The *solid markers* represent the samples that belong to the tested class and should ideally have a class fit value of 1.0. The *open markers* correspond to samples which do not belong to the tested class and ideally have a class fit of 0

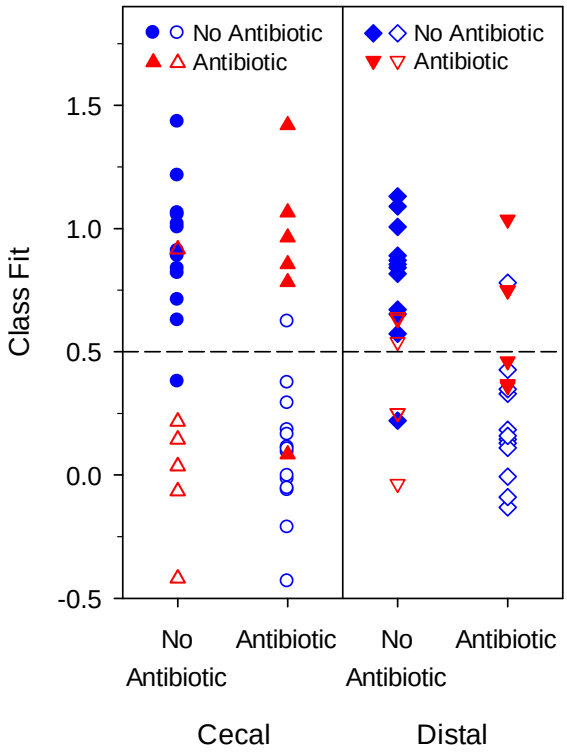

Fig. 6 PLS-DA analysis of cecal and distal colon content verification-set samples for antibiotic treatment, including diets and AOM-treated samples. The *solid markers* represent the samples that belong to the tested class and should ideally have a class fit value of 1.0. The *open markers* correspond to samples that do not belong to the tested class and ideally have a class fit of 0

three, and seven samples from the control, HA7, OS-HA7, and StA-HA7 diets, respectively. The PLS-DA analysis of cecal contents for diet correctly classified all training-set samples; all verification-set samples were classified properly. Figure 5 displays the PLS-DA results and the quality of separation for the cecal contents RS diet groups. The closed and open symbols correspond to verification-set samples that do and do not belong to the indicated diet, respectively. For the control and OS-HA7 diets, all samples were spaced well away from the 0.5 nominal threshold for class differentiation. StA-HA7 had nearly all closed symbols positioned well above the 0.5 line, but one sample appeared slightly above the nominal threshold. HA7 had three of its samples positioned above the 0.5 line, but one sample appeared below the threshold line. Nevertheless, it is readily classified as HA7 because its class-fit values for all of the other diets were even lower.

PLS-DA fingerprint analysis for the cecal contents was also carried out for the antibiotic subgroup treatments. The cecal contents PLS-DA antibiotic analysis had no training-set misclassifications. In Fig. 6, only two verification-set samples were misclassified. Thus, the PLS-DA statistical classification separated the cecal contents antibiotic and saline treatments well.

Classifying the cecal-content samples by AOM subgroup treatment was much less successful (data not shown). PLS-DA was able to produce a model for AOM treatment classification that properly predicted all of the training-set samples, but its analysis yielded 13 misclassifications among the 20 verification-set samples. Clearly, at the time the animals were sacrificed and the samples taken, 8 weeks after the last AOM injection, the AOM treatment had too little effect on the cecal contents to be observed via mass spectrometry.

Statistical analysis of distal colon contents

Classification analysis was also performed for the spectra of the distal colon contents RS groups. PLS-DA was performed with a 54-sample training set and 18-member verification set. The verification set contained six, three, three, and six samples from the control, HA7, OS-HA7, and StA-HA7 diets, respectively. The PLS-DA diet group analysis of the distal colon contents misclassified only one verification-set sample. Figure 7 shows the PLS-DA verification-set analysis of the distal colon contents. The distal-colon-contents categorization for the diet samples was not as clean as it was for the cecal contents. The HA7, OS-HA7, and StA-HA7 diets have all of their markers in the correct region above or below the 0.5 class-fit threshold, but many markers occur very close to the threshold. The control diet classification clearly shows all of the errant samples. In the control diet classification, one control sample fell below the 0.5 class-fit threshold, but it still correctly classified due to its class-fit value being closest to one for the control group. The other errant sample in the control-diet classification is the open, inverted triangle (StA-HA7 sample) at a control-diet class-fit value of 0.76. This same sample corresponds to the highest filled triangle in the StA-HA7 classification (class-fit value 1.45). Because the class-fit value for the sample in the control diet class is closer to one, the sample was misclassified as belonging to the control diet.

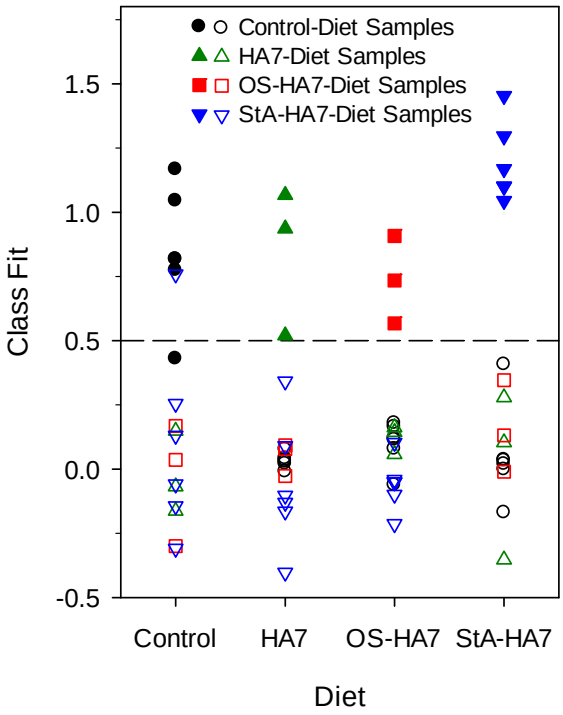

Fig. 7 PLS-DA analysis of distal colon-content verification-set samples for diet treatments, including AOM- and antibiotic-treated samples. The *solid markers* represent the samples that belong to the tested class and should ideally have a class fit value of 1.0. The *open markers* correspond to samples that do not belong to the tested class and ideally have a class fit of 0

PLS-DA analysis of the distal-colon-contents training set for antibiotic treatment had no misclassified samples. The PLS-DA verification set in Fig. 6 contained four misclassified samples. The PLS-DA classification was able only to modestly separate distal colon antibiotic and saline subgroup treatments. It has been observed that antibiotics have a profound effect on the microbial gut community and metabolic processes in mice [42]. A cultured gut microbial community can return to pre-antibiotic treatment levels approximately 3 weeks after treatment [53, 54]. A metabolic study also determined that urinary and fecal metabolites of mice return to near control conditions 3 weeks after antibiotic treatment [55]. However, a comprehensive

pyrosequencing study of the gut microbiome found that antibiotic recovery did not return to the initial conditions, even after 6 weeks [56].

Our findings are consistent with long-term antibiotic perturbations to the gut microbiome. Eight weeks after the antibiotic treatment, the cecal contents antibiotic treatment was still well separated from the saline treatment, and distal colon antibiotic treatment was modestly different from the saline treatment (Fig. 6).

The distal colon PLS-DA modeling of the training set for AOM treatment had no misclassifications. The verification set for the PLS-DA analysis had four misclassifications (data not shown). AOM is a carcinogen and promotes the growth of preneoplastic lesions in the colon. Previous work had suggested that a RS diet decreased the levels of preneoplastic lesions in rats given AOM [47] but preneoplastic lesions in the animals used for this study were not appreciably different among the four diet treatments (unpublished data). As described above, the cecum metabolite profile was not greatly affected by the AOM treatment. The PLS-DA distal colon analysis does appear to show that AOM may have had a minor effect on the metabolite profile in the distal colon. This could be attributed to the possibility that lesions would appear in the colon, rather than the cecum. These lesions thus would most likely not have a large effect upstream on the cecal metabolites.

Biomarkers from resistant starch diets

An effort was made to locate a small group of distinctive metabolites from the cecal and distal colon contents diet treatments as indicators or biomarkers for the diets. The statistical analysis of the cecal and distal colon contents yielded a vector regression plot for each diet (data not shown). The regression vectors indicated how strongly each *m*/*z* peak contributed to the PLS-DA classification of the parent diet in relation to the three diets by assigning each *m*/*z* peak a relative intensity. Mass spectral peaks that contributed a substantial weight to the variation and classification of the diets gave a strong, positive vector intensity for that diet. The absolute normalized intensity of a *m*/*z* peak within a specific diet in relation to the other diets did not necessarily predict a large vector regression coefficient. In many cases, *m*/*z* peaks had analogous intensities among multiple groups, but was considered a biomarker for only a single group. That biomarker had a high regression coefficient because the *m*/*z* peak was a key component in classifying that diet group from the others.

For both cecal and distal colon contents analysis, the five or six metabolites with the strongest positive regression-vector values were examined as potential biomarkers. The accurate *m*/*z* values of these potential biomarkers were compared against the KEGG database using MassTRIX [50]. The accurate mass of the biomarkers matched within an accuracy of ±0.005 Da.

The potential biomarkers from each RS diet for cecal and distal colon contents are shown in Table 2. The biomarkers comprise a variety of compound classes ranging from amino acids and glucose to various steroids. Amino acids appear often among many of the diet categories; proline, leucine, isoleucine, valine, methionine, and phenylalanine are all present. In many cases, the amino acid biomarkers that are prevalent in the cecal contents are not prevalent enough to be chosen as biomarkers for the distal colon contents. The control diet was the only diet to retain an amino acid biomarker, proline, between cecal and distal colon contents. By contrast, the control diet has leucine or isoleucine only in the cecum, while methionine appears only in the distal colon contents list. It is not apparent why the RS diets would have such variations in the

prevalence of amino acid biomarkers, but the large differences between the cecum and the distal colon could be due to host absorption or differences in the bacterial community induced by the different diets. Table 2 also shows that many biomarkers are conserved in both the cecal and distal colon contents. Biomarkers with the *m*/*z* of 116.071, 148.134, 251.128, 321.240, 336.228, 357.239, and 595.352 were observed in the cecal and distal contents in their respective diet groups. The similarity in the biomarkers between the cecal and distal colon contents correspond well with Fig. 4. The Fig. 4 control and StA-HA7 diets contained many of the same cecal and distal-colon contents *m*/*z* peaks. Thus, many of the most prominent biomarkers could transit the large intestine.

Conclusions

Metabolite extracts of rat cecal and distal colon contents from the starch diets could be accurately fingerprinted using PLS-DA. The PLS-DA verification-set plots showed that the diet groups for the cecal and distal colon contents could be distinguished from each other. Utilizing PLS-DA, the antibiotic subgroup treatments were divided well for the cecal contents and modestly separated for the distal colon contents. Thus, the digestive system of the rats had most likely regained normal function following antibiotic treatment, but had different microbial communities. The AOM- and saline-treated rats partially separated based on the distal colon contents, but failed to separate for the cecal contents. The AOM treatment may not have had an effect on the cecum due to AOM targeting the colon or the time frame of AOM-induced carcinogenesis may not have been reached.

Future proposed work will involve studying changes in metabolites over time within the period immediately following administration of the diet. Compounds that appear to change over time will be compared to biomarkers in this study in an attempt to improve understanding of RS digestion. In addition due to the variety of biomarker compounds, parallel companion studies will be run to observe polar or nonpolar metabolites and to definitely identify observed compounds using MS/MS or GC/MS.

Acknowledgement: We would like to thank Dr. Gregory J. Phillips for the use of his lab to extract the fecal metabolites (Department of Veterinary Science and Medicine, Iowa State University). We would also like to give our appreciation to Herman S. Sahota for the use of custom software to average mass spectra (Department of Computer Science, Iowa State University). This project was supported by the Iowa State University Plant Sciences Institute and supported in part by the Department of Agriculture, CSREES award number 2009-65503-05798. This research was performed in part at the Ames Laboratory. Ames Laboratory is operated for the US Department of Energy by Iowa State University under contract no. DE-AC02-07CH11358.

Table 1

Metabolite peaks found in (C) cecal and (D) distal colon samples as shown in Figs. 1, 2, and 3

Peak	*m/z*	Control	HA7	OS-HA7	StA-HA7
a	116.071	D			D
b	118.087	D	C D	C D	C D
c	121.065			C	
d	132.102	C D	C D	C D	C D
e	141.066		C		C
f	141.112	C			C
g	148.134	C D	C		C D
h	166.087	C D		C D	C D
i	173.129		C		C
j	195.113		C D		C D
k	212.14		C	C	C D
l	217.104				D
m	229.151			D	
n	230.187		C D		C D
o	242.187				D
p	251.128			C D	
q	273.108			D	
r	276.134		C D		C D
s	277.129		C D	C	C D
t	321.240				C D
u	335.219				C
v	336.228		D		D
w	357.239			C D	
x	373.274	D			D
y	377.265	C			
z	378.269	C			
aa	379.280	C			
ab	393.242	C	C		
ac	409.164				D
ad	479.263			C D	
ae	501.246			D	
af	563.268		D		
ag	591.322			C	
ah	595.352	D			C D
ai	733.559	C			
aj	737.286			C D	
ak	839.565				C D

Table 2

Biomarkers with substantial contribution to class differentiation matched to KEGG Database

Cecal contents	*m/z*	Compound[a]	Molecular Formula
Control	116.071	Proline $[M+H]^+$	$C_5H_9NO_2$
	132.102	Leucine $[M+H]^+$	$C_6H_{13}NO_2$
	132.102	Isoleucine $[M+H]^+$	$C_6H_{13}NO_2$
	148.134	No database match	Unknown
	377.265	3-acetyl-5alpha-androstane-3beta,17beta-diol 3-acetate $[M+H]^+$	$C_{23}H_{36}O_4$
	595.350	L-Stercobilin $[M+H]^+$	$C_{33}H_{46}N_4O_6$
HA7 diet	118.087	Valine $[M+H]^+$	$C_5H_{11}NO_2$
	141.113	2-Methylcholine $[M+Na]^+$	$C_6H_{16}NO$
	161.093	Alanyl-alanine $[M+H]^+$	$C_6H_{12}N_2O_3$
	161.093	Nonadienal $[M+Na]^+$	$C_9H_{14}O$
	203.053	Glucose $[M+Na]^+$	$C_6H_{12}O_6$
	336.228	12-hydroxyicosa-trienoic acid $[M+H]^+$	$C_{20}H_{31}O_4$
OS-HA7	251.129	Methylripariochromene A $[M+H]^+$	$C_{14}H_{18}O_4$
	294.157	No database match	Unknown
	357.238	Allotetrahydrodeoxycorticosterone $[M+Na]^+$	$C_{21}H_{34}O_3$
	479.263	No database match	Unknown
	591.322	Urobilin $[M+H]^+$	$C_{33}H_{42}N_4O_6$
	591.322	Deoxycholic acid 3-glucuronide $[M+Na]^+$	$C_{30}H_{48}O_{10}$
StA-HA7	242.187	No database match	$C_{17}H_{23}N$
	276.134	Alanyltryptophan $[M+H]^+$	$C_{14}H_{17}N_3O_3$
	277.129	Homoanserine $[M+Na]^+$	$C_{11}H_{18}N_4O_3$
	321.240	Oxooctadecanoic acid $[M+Na]^+$	$C_{18}H_{34}O_3$
	321.240	Hydroxy-eicosatetraenoic acid $[M+H]^+$	$C_{20}H_{32}O_3$
	335.219	Hydroperoxy, octadecadienoic acid $[M+Na]^+$	$C_{18}H_{32}O_4$

Distal contents	*m/z*	Compound[a]	Molecular Formula
Control	116.071	Proline $[M+H]^+$	$C_5H_9NO_2$
	141.111	2-Methylcholine $[M+Na]^+$	$C_6H_{16}NO$
	148.134	No database match	Unknown
	150.059	Methionine $[M+H]^+$	$C_5H_{11}NO_2S$
	595.353	L-Stercobilin $[M+H]^+$	$C_{33}H_{46}N_4O_6$
HA7 diet	230.187	No database match	Unknown
	254.155	Gamma-aminobutyryl-lysine $[M+Na]^+$	$C_{10}H_{21}N_3O_3$
	255.147	Homoanserine $[M+H]^+$	$C_{11}H_{18}N_4O_3$
	336.228	12-Hydroxyicosa-trienoic acid $[M+H]^+$	$C_{20}H_{31}O_4$
	563.268	Protoporphyrin $[M+Na]^+$	$C_{34}H_{34}N_4O_4$

OS-HA7	118.087	Valine $[M+H]^+$	$C_5H_{11}NO_2$
	212.140	No database match	Unknown
	251.127	Methylripariochromene A $[M+H]^+$	$C_{14}H_{18}O_4$
	294.162	No database match	Unknown
	357.240	Allotetrahydrodeoxycorticosterone $[M+Na]^+$	$C_{21}H_{34}O_3$
	737.286	No database match	Unknown
StA-HA7	116.071	Proline $[M+H]^+$	$C_5H_9NO_2$
	124.039	Picolinic acid $[M+H]^+$	$C_6H_5NO_2$
	166.087	Phenylalanine $[M+H]^+$	$C_9H_{11}NO_2$
	166.087	Stachydrine $[M+Na]^+$	$C_7H_{13}NO_2$
	212.140	No database match	Unknown
	321.240	Oxooctadecanoic acid $[M+Na]^+$	$C_{18}H_{34}O_3$
	321.240	Hydroxy-eicosatetraenoic acid $[M+H]^+$	$C_{20}H_{32}O_3$
	409.164	Burseran $[M+Na]^+$	$C_{22}H_{26}O_6$
	409.164	1,2-Dihydro-5-hydroxy-2-(1-hydroxy-1-methylethyl)-4-(isobutyryl)-6-phenylfurano [2,3-h][1]benzopyran-8-one $[M+H]^+$	$C_{24}H_{24}O_6$

[a]Notation refers to the stated molecule (M) and the observed adduct bracketed with the positive charge

References

1. Sajilata MG, Singhal RS, Kulkarni PR (2006) Resistant starch–a review. Compr Rev Food Sci Food Saf 5:1-17
2. Atkin NJ, Cheng SL, Abeysekera RM, Robards AW (1999) Localisation of amylose and amylopectin in starch granules using enzyme-gold labelling. Starch-Stärke 51:163-172
3. Jane J (2009) In: BeMiller JN, Whistler RL (eds) Starch: chemistry and technology; 3rd edn. Academic, Orlando
4. Champ M, Langkilde A-M, Brouns F, Kettlitz B, Le Bail-Collet Y (2003) Advances in dietary fibre characterisation. 2. Consumption, chemistry, physiology and measurement of resistant starch; implications for health and food labeling. Nutr Res Rev 16:143-161
5. Robertson MD (2012) Dietary-resistant starch and glucose metabolism. Curr Opin Clin Nutr Metab Care 15:362-367
6. Saltiel AR, Kahn CR (2001) Insulin signalling and the regulation of glucose and lipid metabolism. Nature 414:799-806
7. Ranganathan S, Champ M, Pechard C, Blanchard P, Nguyen M, Colonna P, Krempf M (1994) Comparative study of the acute effects of resistant starch and dietary fibers on metabolic indexes in men. Am J Clin Nutr 59:879-883
8. Eckel RH, Grundy SM, Zimmet PZ (2005) The metabolic syndrome. Lancet 365:1415-1428
9. Bodinham CL, Frost GS, Robertson MD (2010) Acute ingestion of resistant starch reduces food intake in healthy adults. Brit J Nutr 103:917-922
10. Gibson GR, Probert HM, Van Loo J, Rastall RA, Roberfroid MB (2004) Dietary modulation of the human colonic microbiota: updating the concept of prebiotics. Nutr Res Rev 17:259-275

11. Jenkins DJA, Vuksan V, Kendall CWC, Würsch P, Jeffcoat R, Waring S, Mehling CC, Vidgen E, Augustin LSA, Wong E (1998) Physiological effects of resistant starches on fecal bulk, short chain fatty acids, blood lipids and glycemic index. J Am Coll Nutr 17: 609-616
12. Nilsson AC, Östman EM, Knudsen KEB, Holst JJ, Björck IME (2010) A cereal-based evening meal rich in indigestible carbohydrates increases plasma butyrate the next morning. J Nutr 140:1932-1936
13. Ding S, Chi MM, Scull BP, Rigby R, Schwerbrock NMJ, Magness S, Jobin C, Lund PK (2010) High-fat diet: bacteria interactions promote intestinal inflammation which precedes and correlates with obesity and insulin resistance in mouse. PLOS One 5:e12191
14. Brown IL, Wang X, Topping DL, Playne MJ, Conway PL (1998) High amylose maize starch as a versatile prebiotic for use with probiotic bacteria. Food Aust 50:603-610
15. Roberfroid MB (2002) Functional foods: concepts and applications to inulin and oligofructose. Br J Nutr 87:S139-S143
16. Tuohy KM, Ziemer CJ, Klinder A, Knöbel Y, Pool-Zobel BL, Gibson GR (2002) A human volunteer study to determine the prebiotic effects of lactulose powder on human colonic microbiota. Microb Ecol Health Dis 14:165-173
17. Ito M, Kimura M, Deguchi Y, Miyamori-Watabe A, Yajima T, Kan T (1993) Effects of transgalactosylated disaccharides on the human intestinal microflora and their metabolism. J Nutr Sci Vitaminol 39:279-288
18. Marotti I, Bregola V, Aloisio I, Di Gioia D, Bosi S, Di Silvestro R, Quinn R, Dinelli G (2012) Prebiotic effect of soluble fibres from modern and old durum-type wheat varieties on *Lactobacillus* and *Bifidobacterium* strains. J Sci Food Agric 92:2133-2140
19. Kritchevsky D (1995) Epidemiology of fibre, resistant starch and colorectal cancer. Eur J Cancer Prev 4:345-352
20. van Munster IP, Tangerman A, Nagengast FM (1994) Effect of resistant starch on colonic fermentation, bile acid metabolism, and mucosal proliferation. Dig Dis Sci 39:834-842
21. Hamer HM, De Preter V, Windey K, Verbeke K (2012) Functional analysis of colonic bacterial metabolism: relevant to health? Am J Physiol Gastrointest Liver Physiol 302:G1-G9
22. Yin P, Zhao X, Li Q, Wang J, Li J, Xu G (2006) Metabonomics study of intestinal fistulas based on ultraperformance liquid chromatography coupled with Q-TOF mass spectrometry (UPLC/Q-TOF MS). J Proteome Res 5:2135-2143
23. Williams RE, Lenz EM, Evans JA, Wilson ID, Granger JH, Plumb RS, Stumpf CL (2005) A combined ^{1}H NMR and HPLC-MS-based metabonomic study of urine from obese (fa/fa) Zucker and normal Wistar-derived rats. J Pharm Biomed Anal 38:465-471
24. Poroyko V, Morowitz M, Bell T, Ulanov A, Wang M, Donovan S, Bao N, Gu S, Hong L, Alverdy JC, Bergelson J, Liu DC (2011) Diet creates metabolic niches in the "inmature gut" that shape microbial communities. Nutr Hosp 26:1283-1295
25. Mellert W, Kapp M, Strauss V, Wiemer J, Kamp H, Walk T, Looser R, Prokoudine A, Fabian E, Krennrich G, Herold M, van Ravenzwaay B (2011) Nutritional impact on the plasma metabolome of rats. Toxicol Lett 207:173-181
26. Legido-Quigley C, Stella C, Perez-Jimenez F, Lopez-Miranda J, Ordovas J, Powell J, van-der-Ouderaa F, Ware L, Lindon JC, Nicholson JK, Holmes E (2010) Liquid chromatography-mass spectrometry methods for urinary biomarker detection in metabonomic studies with application to nutritional studies. Biomed Chromatogr 24:737-743

27. Ventura M, Turroni F, Canchaya C, Vaughan EE, O'Toole PW, van Sinderen D (2009) Microbial diversity in the human intestine and novel insights from metagenomics. Front Biosci 14:3214-3221
28. Englyst HN, Kingman SM, Cumming JH (1992) Classification and measurement of nutritionally important starch fractions. Eur J Clin Nutr 46:S33-S50
29. Baghurst PA, Baghurst KI, Record SJ (1996) Dietary fibre, non-starch polysaccharides and resistant starch–a review. Food Aust 48:S3-S35
30. Hasjim J, Lee S-O, Hendrich S, Setiawan S, Ai Y, Jane J (2010) Characterization of novel resistant-starch and its effects on postprandial plasma-glucose and insulin responses. Cereal Chem 87:257-262
31. Dettmer K, Aronov PA, Hammock BD (2007) Mass spectrometry-based metabolomics. Mass Spectrom Rev 26:51-78
32. Scalbert A, Brennan L, Fiehn O, Hankemeier T, Kristal BS, van Ommen B, Pujos-Guillot E, Verheij E, Wishart D, Wopereis S (2009) Mass-spectrometry-based metabolomics: limitations and recommendations for future progress with particular focus on nutrition research. Metabolomics 5:435-458
33. Vitali B, Ndagijimana M, Maccaferri S, Biagi E, Guerzoni ME, Brigidi P (2012) An in vitro evaluation of the effect of probiotics and prebiotics on the metabolic profile of human microbiota. Anaerobe 18:386-391
34. Blokland MH, Van Tricht EF, Van Rossum HJ, Sterk SS, Nielen MWF (2012) Endogenous steroid profiling by gas chromatography-tandem mass spectrometry and multivariate statistics for the detection of natural hormone abuse in cattle. Food Addit Contam A 29:1030-1045
35. Tsugawa H, Tsujimoto Y, Arita M, Bamba T, Fukusaki E (2011) GC/MS based metabolomics: development of a data mining system for metabolite identification by using soft independent modeling of class analogy (SIMCA). BMC Bioinformatics 12:131
36. Plumb RS, Granger JH, Stumpf CL, Johnson KA, Smith BW, Gaulitz S, Wilson ID, Castro-Perez J (2005) A rapid screening approach to metabonomics using UPLC and oa-TOF mass spectrometry: application to age, gender and diurnal variation in normal/Zucker obese rats and black, white and nude mice. Analyst 130:844-849
37. Mateos-Martín ML, Pérez-Jiménez J, Fuguet E, Torres JL (2012) Non-extractable proanthocyanidins from grapes are a source of bioavailable (epi)catechin and derived metabolites in rats. Br J Nutr 108:290-297
38. Ohashi Y, Hirayama A, Ishikawa T, Nakamura S, Shimizu K, Ueno Y, Tomita M, Soga T (2008) Depiction of metabolome changes in histidine-starved *Escherichia coli* by CE-TOFMS. Mol Biosyst 4:135-147
39. Matsumoto M, Kibe R, Ooga T, Aiba Y, Kurihara S, Sawaki E, Koga Y, Benno Y (2012) Impact of intestinal microbiota on intestinal luminal metabolome. Sci Rep 2:233
40. Ooga T, Sato H, Nagashima A, Sasaki K, Tomita M, Soga T, Ohashi Y (2011) Metabolomic anatomy of an animal model revealing homeostatic imbalances in dyslipidaemia. Mol Biosyst 7:1217-1223
41. Hasegawa M, Ide M, Kuwamura M, Yamate J, Takenaka S (2010) Metabolic fingerprinting in toxicological assessment using FT-ICR MS. J Toxicol Pathol 23:67-74
42. Antunes LCM, Han J, Ferreira RBR, Lolić P, Borchers CH, Finlay BB (2011) Effect of antibiotic treatment on the intestinal metabolome. Antimicrob Agents Chemother 55:1494-1503

43. Rath CM, Alexandrov T, Higginbottom SK, Song J, Milla ME, Fischbach MA, Sonnenburg JL, Dorrestein PC (2012) Molecular analysis of model gut microbiotas by imaging mass spectrometry and nanodesorption electrospray ionization reveals dietary metabolite transformations. Anal Chem 84:9259-9267
44. Chen Y, Zhu SB, Xie MY, Nie SP, Liu W, Li C, Gong XF, Wang YX (2008) Quality control and original discrimination of Ganoderma lucidum based on high-performance liquid chromatographic fingerprints and combined chemometrics methods. Anal Chim Acta 623:146-156
45. Fremout W, Kuckova S, Crhova M, Sanyova J, Saverwyns S, Hynek R, Kodicek M, Vandenabeele P, Moens L (2011) Classification of protein binders in artist's paints by matrix-assisted laser desorption/ionisation time-of-flight mass spectrometry: an evaluation of principal component analysis (PCA) and soft independent modeling of class analogy (SIMCA). Rapid Commun Mass Spectrom 25:1631-1640
46. Benabdelkamel H, Di Donna L, Mazzotti F, Naccarato A, Sindona G, Tagarelli A, Taverna D (2012) Authenticity of PGI "Clementine of Calabria" by multielement fingerprint. J Agric Food Chem 60:3717-3726
47. Zhao Y, Hasjim J, Li L, Jane J, Hendrich S, Birt DF (2011) Inhibition of azoxymethane-induced preneoplastic lesions in the rat colon by a cooked stearic acid complexed high-amylose cornstarch. J Agric Food Chem 59:9700-9708
48. Reeves PG (1997) Components of the AIN-93 diets as improvements in the AIN-76A diet. J Nutr 127:838S-841S
49. Zhang B, Huang Q, Luo F, Fu X, Jiang H, Jane J (2011) Effects of octenylsuccinylation on the structure and properties of high-amylose maize starch. Carbohyd Polym 84:1276-1281
50. Suhre K, Schmitt-Kopplin P (2008) MassTRIX: mass translator into pathways. Nucleic Acids Res 36:W481-W484 (Web Server Issue)
51. Westerhuis JA, de Jong S, Smilde AK (2001) Direct orthogonal signal correction. Chemometr Intell Lab Syst 56:13-25
52. Anderson TJ, Ai Y, Jones RW, Houk RS, Jane J, Zhao Y, Birt DF, McClelland JF (2013) Analysis of resistant starches in rat cecal contents using Fourier transform infrared photoacoustic spectroscopy. J Agric Food Chem 61:1818-1822
53. Croswell A, Amir E, Teggatz P, Barman M, Salzman NH (2009) Prolonged impact of antibiotics on intestinal microbial ecology and susceptibility to enteric *Salmonella* infection. Infect Immun 77:2741-2753
54. Manichanh C, Reeder J, Gibert P, Varela E, Llopis M, Antolin M, Guigo R, Knight R, Guarner F (2010) Reshaping the gut microbiome with bacterial transplantation and antibiotic intake. Genome Res 20:1411-1419
55. Zhung X, Xie G, Zhao A, Zhao L, Yao C, Chiu NHL, Zhou Z, Bao Y, Jia W, Nicholson JK, Jia W (2011) The footprints of gut microbial-mammalian co-metabolism. J Proteome Res 10:5512-5522
56. Antonopoulos DA, Huse SM, Morrison HG, Schmidt TM, Sogin ML, Young VB (2009) Reproducible community dynamics of the gastrointestinal microbiota following antibiotic perturbation. Infect Immun 77:2367-2375.